

DESY-04-164
September 2004

Search for a narrow charmed baryonic state decaying to $D^{*\pm}p^\mp$ in ep collisions at HERA

ZEUS Collaboration

Abstract

A resonance search has been made in the $D^{*\pm}p^\mp$ invariant-mass spectrum with the ZEUS detector at HERA using an integrated luminosity of 126 pb^{-1} . The decay channels $D^{*+} \rightarrow D^0\pi_s^+ \rightarrow (K^-\pi^+)\pi_s^+$ and $D^{*+} \rightarrow D^0\pi_s^+ \rightarrow (K^-\pi^+\pi^+\pi^-)\pi_s^+$ (and the corresponding antiparticle decays) were used to identify $D^{*\pm}$ mesons. No resonance structure was observed in the $D^{*\pm}p^\mp$ mass spectrum from more than 60 000 reconstructed $D^{*\pm}$ mesons. The results are not compatible with a report of the H1 Collaboration of a charmed pentaquark, Θ_c^0 .

The ZEUS Collaboration

S. Chekanov, M. Derrick, J.H. Loizides¹, S. Magill, S. Miglioranzi¹, B. Musgrave, J. Repond, R. Yoshida

Argonne National Laboratory, Argonne, Illinois 60439-4815, USA ⁿ

M.C.K. Mattingly

Andrews University, Berrien Springs, Michigan 49104-0380, USA

N. Pavel

Institut für Physik der Humboldt-Universität zu Berlin, Berlin, Germany

P. Antonioli, G. Bari, M. Basile, L. Bellagamba, D. Boscherini, A. Bruni, G. Bruni, G. Cara Romeo, L. Cifarelli, F. Cindolo, A. Contin, M. Corradi, S. De Pasquale, P. Giusti, G. Iacobucci, A. Margotti, A. Montanari, R. Nania, F. Palmonari, A. Pesci, A. Polini, L. Rinaldi, G. Sartorelli, A. Zichichi

University and INFN Bologna, Bologna, Italy ^e

G. Aghuzumtsyan, D. Bartsch, I. Brock, S. Goers, H. Hartmann, E. Hilger, P. Irrgang, H.-P. Jakob, O. Kind, U. Meyer, E. Paul², J. Rautenberg, R. Renner, K.C. Voss, M. Wang
Physikalisches Institut der Universität Bonn, Bonn, Germany ^b

D.S. Bailey³, N.H. Brook, J.E. Cole, G.P. Heath, T. Namsoo, S. Robins, M. Wing
H.H. Wills Physics Laboratory, University of Bristol, Bristol, United Kingdom ^m

M. Capua, A. Mastroberardino, M. Schioppa, G. Susinno
Calabria University, Physics Department and INFN, Cosenza, Italy ^e

J.Y. Kim, K.J. Ma
Chonnam National University, Kwangju, South Korea ^g

M. Helbich, Y. Ning, Z. Ren, W.B. Schmidke, F. Sciulli
Nevis Laboratories, Columbia University, Irvington on Hudson, New York 10027 ^o

J. Chwastowski, A. Eskreys, J. Figiel, A. Galas, K. Olkiewicz, P. Stopa, D. Szuba, L. Zawiejski
Institute of Nuclear Physics, Cracow, Poland ⁱ

L. Adamczyk, T. Bołd, I. Grabowska-Bołd⁴, D. Kisiełwska, A.M. Kowal, J. Łukasik, M. Przybycień, L. Suszycki, J. Szuba⁵
Faculty of Physics and Applied Computer Science, AGH-University of Science and Technology, Cracow, Poland ^p

A. Kotański⁶, W. Słomiński
Department of Physics, Jagellonian University, Cracow, Poland

V. Adler, U. Behrens, I. Bloch, K. Borras, D. Dannheim⁷, G. Drews, J. Fourletova, U. Fricke, A. Geiser, D. Gladkov, P. Göttlicher⁸, O. Gutsche, T. Haas, W. Hain, C. Horn, B. Kahle, U. Kötz, H. Kowalski, G. Kramberger, H. Labes, D. Lelas⁹, H. Lim, B. Löhr, R. Mankel, I.-A. Melzer-Pellmann, C.N. Nguyen, D. Notz, A.E. Nuncio-Quiroz, A. Raval, R. Santamarta, U. Schneekloth, A. Stifutkin, U. Stösslein, G. Wolf, C. Youngman, W. Zeuner
Deutsches Elektronen-Synchrotron DESY, Hamburg, Germany

S. Schlenstedt
Deutsches Elektronen-Synchrotron DESY, Zeuthen, Germany

G. Barbagli, E. Gallo, C. Genta, P. G. Pelfer
University and INFN, Florence, Italy^e

A. Bamberger, A. Benen, F. Karstens, D. Dobur, N.N. Vlasov¹⁰
Fakultät für Physik der Universität Freiburg i.Br., Freiburg i.Br., Germany^b

P.J. Bussey, A.T. Doyle, J. Ferrando, J. Hamilton, S. Hanlon, D.H. Saxon, I.O. Skillicorn
Department of Physics and Astronomy, University of Glasgow, Glasgow, United Kingdom^m

I. Gialas¹¹
Department of Engineering in Management and Finance, Univ. of Aegean, Greece

T. Carli, T. Gosau, U. Holm, N. Krumnack, E. Lohrmann, M. Milite, H. Salehi, P. Schleper, T. Schörner-Sadenius, S. Stonjek¹², K. Wichmann, K. Wick, A. Ziegler, Ar. Ziegler
Hamburg University, Institute of Exp. Physics, Hamburg, Germany^b

C. Collins-Tooth¹³, C. Foudas, R. Gonçalo¹⁴, K.R. Long, A.D. Tapper
Imperial College London, High Energy Nuclear Physics Group, London, United Kingdom^m

P. Cloth, D. Filges
Forschungszentrum Jülich, Institut für Kernphysik, Jülich, Germany

M. Kataoka¹⁵, K. Nagano, K. Tokushuku¹⁶, S. Yamada, Y. Yamazaki
Institute of Particle and Nuclear Studies, KEK, Tsukuba, Japan^f

A.N. Barakbaev, E.G. Boos, N.S. Pokrovskiy, B.O. Zhautykov
Institute of Physics and Technology of Ministry of Education and Science of Kazakhstan, Almaty, Kazakhstan

D. Son
Kyungpook National University, Center for High Energy Physics, Daegu, South Korea^g

J. de Favereau, K. Piotrkowski
Institut de Physique Nucléaire, Université Catholique de Louvain, Louvain-la-Neuve, Belgium^q

F. Barreiro, C. Glasman¹⁷, O. González, L. Labarga, J. del Peso, E. Tassi, J. Terrón,
M. Zambrana

Departamento de Física Teórica, Universidad Autónoma de Madrid, Madrid, Spain^l

M. Barbi, F. Corriveau, C. Liu, S. Padhi, M. Plamondon, D.G. Stairs, R. Walsh, C. Zhou
Department of Physics, McGill University, Montréal, Québec, Canada H3A 2T8^a

T. Tsurugai

Meiji Gakuin University, Faculty of General Education, Yokohama, Japan^f

A. Antonov, P. Danilov, B.A. Dolgoshein, V. Sosnovtsev, S. Suchkov

Moscow Engineering Physics Institute, Moscow, Russia^j

R.K. Dementiev, P.F. Ermolov, I.I. Katkov, L.A. Khein, I.A. Korzhavina, V.A. Kuzmin,
B.B. Levchenko, O.Yu. Lukina, A.S. Proskuryakov, L.M. Shcheglova, S.A. Zotkin

Moscow State University, Institute of Nuclear Physics, Moscow, Russia^k

I. Abt, C. Büttner, A. Caldwell, X. Liu, J. Sutiak

Max-Planck-Institut für Physik, München, Germany

N. Coppola, G. Grigorescu, S. Griepink, A. Keramidas, E. Koffeman, P. Kooijman,
E. Maddox, A. Pellegrino, S. Schagen, H. Tiecke, M. Vázquez, L. Wiggers, E. de Wolf

NIKHEF and University of Amsterdam, Amsterdam, Netherlands^h

N. Brümmer, B. Bylsma, L.S. Durkin, T.Y. Ling

*Physics Department, Ohio State University, Columbus, Ohio 43210*ⁿ

P.D. Allfrey, M.A. Bell, A.M. Cooper-Sarkar, A. Cottrell, R.C.E. Devenish, B. Foster,
G. Grzelak, C. Gwenlan¹⁸, T. Kohno, S. Patel, P.B. Straub, R. Walczak

Department of Physics, University of Oxford, Oxford United Kingdom^m

P. Bellan, A. Bertolin, R. Brugnera, R. Carlin, R. Ciesielski, F. Dal Corso, S. Dusini,
A. Garfagnini, S. Limentani, A. Longhin, A. Parenti, M. Posocco, L. Stanco, M. Turcato

Dipartimento di Fisica dell' Università and INFN, Padova, Italy^e

E.A. Heaphy, F. Metlica, B.Y. Oh, J.J. Whitmore¹⁹

*Department of Physics, Pennsylvania State University, University Park, Pennsylvania
16802*^o

Y. Iga

Polytechnic University, Sagamihara, Japan^f

G. D'Agostini, G. Marini, A. Nigro

Dipartimento di Fisica, Università 'La Sapienza' and INFN, Rome, Italy^e

J.C. Hart

Rutherford Appleton Laboratory, Chilton, Didcot, Oxon, United Kingdom^m

C. Heusch

University of California, Santa Cruz, California 95064, USA ⁿ

I.H. Park²⁰

Department of Physics, Ewha Womans University, Seoul, Korea

H. Abramowicz²¹, A. Gabareen, S. Kananov, A. Kreisel, A. Levy

Raymond and Beverly Sackler Faculty of Exact Sciences, School of Physics, Tel-Aviv University, Tel-Aviv, Israel ^d

M. Kuze

Department of Physics, Tokyo Institute of Technology, Tokyo, Japan ^f

S. Kagawa, T. Tawara

Department of Physics, University of Tokyo, Tokyo, Japan ^f

R. Hamatsu, H. Kaji, S. Kitamura²², K. Matsuzawa, O. Ota, Y.D. Ri

Tokyo Metropolitan University, Department of Physics, Tokyo, Japan ^f

M. Costa, M.I. Ferrero, V. Monaco, R. Sacchi, A. Solano

Università di Torino and INFN, Torino, Italy ^e

M. Arneodo, M. Ruspa

Università del Piemonte Orientale, Novara, and INFN, Torino, Italy ^e

S. Fourletov, T. Koop, J.F. Martin, A. Mirea

Department of Physics, University of Toronto, Toronto, Ontario, Canada M5S 1A7 ^a

J.M. Butterworth²³, R. Hall-Wilton, T.W. Jones, M.R. Sutton³, C. Targett-Adams

Physics and Astronomy Department, University College London, London, United Kingdom ^m

J. Ciborowski²⁴, P. Łuźniak²⁵, R.J. Nowak, J.M. Pawlak, J. Sztuk²⁶, T. Tymieniecka,

A. Ukleja, J. Ukleja²⁷, A.F. Żarnecki

Warsaw University, Institute of Experimental Physics, Warsaw, Poland

M. Adamus, P. Plucinski

Institute for Nuclear Studies, Warsaw, Poland

Y. Eisenberg, D. Hochman, U. Karshon, M.S. Lightwood, M. Riveline

Department of Particle Physics, Weizmann Institute, Rehovot, Israel ^c

A. Everett, L.K. Gladilin²⁸, D. Kçira, S. Lammers, L. Li, D.D. Reeder, M. Rosin, P. Ryan,

A.A. Savin, W.H. Smith

Department of Physics, University of Wisconsin, Madison, Wisconsin 53706, USA ⁿ

S. Dhawan

Department of Physics, Yale University, New Haven, Connecticut 06520-8121, USA ⁿ

S. Bhadra, C.D. Catterall, G. Hartner, S. Menary, U. Noor, M. Soares, J. Standage,
J. Whyte, C. Ying

Department of Physics, York University, Ontario, Canada M3J 1P3^a

- ¹ also affiliated with University College London, UK
- ² retired
- ³ PPARC Advanced fellow
- ⁴ partly supported by Polish Ministry of Scientific Research and Information Technology, grant no. 2P03B 12225
- ⁵ partly supported by Polish Ministry of Scientific Research and Information Technology, grant no.2P03B 12625
- ⁶ supported by the Polish State Committee for Scientific Research, grant no. 2 P03B 09322
- ⁷ now at Columbia University, N.Y., USA
- ⁸ now at DESY group FEB, Hamburg, Germany
- ⁹ now at LAL, Université de Paris-Sud, IN2P3-CNRS, Orsay, France
- ¹⁰ partly supported by Moscow State University, Russia
- ¹¹ also affiliated with DESY
- ¹² now at University of Oxford, UK
- ¹³ now at the Department of Physics and Astronomy, University of Glasgow, UK
- ¹⁴ now at Royal Holloway University of London, UK
- ¹⁵ also at Nara Women's University, Nara, Japan
- ¹⁶ also at University of Tokyo, Japan
- ¹⁷ Ramón y Cajal Fellow
- ¹⁸ PPARC Postdoctoral Research Fellow
- ¹⁹ on leave of absence at The National Science Foundation, Arlington, VA, USA
- ²⁰ supported by the Intramural Research Grant of Ewha Womans University, South Korea
- ²¹ also at Max Planck Institute, Munich, Germany, Alexander von Humboldt Research Award
- ²² present address: Tokyo Metropolitan University of Health Sciences, Tokyo 116-8551, Japan
- ²³ also at University of Hamburg, Germany, Alexander von Humboldt Fellow
- ²⁴ also at Łódź University, Poland
- ²⁵ Łódź University, Poland
- ²⁶ Łódź University, Poland, supported by the KBN grant 2P03B12925
- ²⁷ supported by the KBN grant 2P03B12725
- ²⁸ on leave from Moscow State University, Russia, partly supported by the Weizmann Institute via the U.S.-Israel Binational Science Foundation

- ^a supported by the Natural Sciences and Engineering Research Council of Canada (NSERC)
- ^b supported by the German Federal Ministry for Education and Research (BMBF), under contract numbers HZ1GUA 2, HZ1GUB 0, HZ1PDA 5, HZ1VFA 5
- ^c supported in part by the MINERVA Gesellschaft für Forschung GmbH, the Israel Science Foundation (grant no. 293/02-11.2), the U.S.-Israel Binational Science Foundation and the Benoziyo Center for High Energy Physics
- ^d supported by the German-Israeli Foundation and the Israel Science Foundation
- ^e supported by the Italian National Institute for Nuclear Physics (INFN)
- ^f supported by the Japanese Ministry of Education, Culture, Sports, Science and Technology (MEXT) and its grants for Scientific Research
- ^g supported by the Korean Ministry of Education and Korea Science and Engineering Foundation
- ^h supported by the Netherlands Foundation for Research on Matter (FOM)
- ⁱ supported by the Polish State Committee for Scientific Research, grant no. 620/E-77/SPB/DESY/P-03/DZ 117/2003-2005 and grant no. 1P03B07427/2004-2006
- ^j partially supported by the German Federal Ministry for Education and Research (BMBF)
- ^k supported by RF President grant N 1685.2003.2 for the leading scientific schools and by the Russian Ministry of Industry, Science and Technology through its grant for Scientific Research on High Energy Physics
- ^l supported by the Spanish Ministry of Education and Science through funds provided by CICYT
- ^m supported by the Particle Physics and Astronomy Research Council, UK
- ⁿ supported by the US Department of Energy
- ^o supported by the US National Science Foundation
- ^p supported by the Polish Ministry of Scientific Research and Information Technology, grant no. 112/E-356/SPUB/DESY/P-03/DZ 116/2003-2005 and 1 P03B 065 27
- ^q supported by FNRS and its associated funds (IISN and FRiA) and by an Inter-University Attraction Poles Programme subsidised by the Belgian Federal Science Policy Office

1 Introduction

The observation of a narrow strange baryonic state decaying to K^+n or K_s^0p has been reported by several experiments [1]. This state has both baryon number and strangeness of +1. Thus the resonance cannot be composed of three quarks but could be explained as a bound state of five quarks: $\Theta^+ = uud\bar{d}\bar{s}$. Evidence for two other pentaquark states with strangeness of -2 has also been reported recently [2]. Although no strange pentaquark production has been observed in some searches [3], the existence of Θ^+ is supported by recent results obtained in ep collisions at HERA [4]. Several QCD models are able to explain the nature of the strange pentaquarks [5–7].

The expected properties of charmed pentaquark states have been discussed in the literature [6, 8–10]. The lightest charmed pentaquark would be $\Theta_c^0 = uud\bar{d}\bar{c}$. In predictions based on the diquark-diquark-antiquark model of Jaffe and Wilzcek [6], the mass of Θ_c^0 is typically below the sum of the masses of the D^- meson and proton. In this case, Θ_c^0 should decay weakly to, e.g., $\Theta^+\pi^-$. Predictions utilising the diquark-triquark model of Karliner and Lipkin [9] suggest a heavier Θ_c^0 decaying dominantly to D^-p . If the mass of the Θ_c^0 were sufficiently large, it could also decay to $D^{*-}p$; there is a possibility that this decay mode is dominant [11].

The observation of a narrow charmed baryonic resonance decaying to $D^{*\pm}p^\mp$ has recently been reported by the H1 Collaboration [12]. A peak containing 50.6 ± 11.2 events was observed in deep inelastic scattering (DIS) with exchanged photon virtuality $Q^2 > 1 \text{ GeV}^2$ at a mass of $3099 \pm 3(\text{stat.}) \pm 5(\text{syst.}) \text{ MeV}$ and with a Gaussian width of $12 \pm 3(\text{stat.}) \text{ MeV}$, compatible with the experimental resolution. A signal with compatible mass and width was also observed in photoproduction ($Q^2 \lesssim 1 \text{ GeV}^2$). The observed resonance was claimed to contribute roughly 1% to the total $D^{*\pm}$ production rate in the kinematic region studied.

This paper presents results of a search for narrow states in the $D^{*\pm}p^\mp$ decay channel in $e^\pm p$ collisions at HERA using the ZEUS detector.

2 Experimental set-up

The analysis was performed with the data taken by the ZEUS Collaboration from 1995 to 2000. In this period, HERA collided electrons or positrons¹ with energy $E_e = 27.5 \text{ GeV}$ and protons with energy $E_p = 820 \text{ GeV}$ (1995–1997) or $E_p = 920 \text{ GeV}$ (1998–2000). The data used in this analysis correspond to an integrated luminosity of $126.5 \pm 2.4 \text{ pb}^{-1}$.

¹ From now on, the word “electron” is used as a generic term for electrons and positrons.

A detailed description of the ZEUS detector can be found elsewhere [13]. A brief outline of the components most relevant to this analysis is given below.

Charged particles are tracked in the central tracking detector (CTD) [14], which operates in a magnetic field of 1.43 T provided by a thin superconducting solenoid. The CTD consists of 72 cylindrical drift chamber layers, organized in nine superlayers covering the polar-angle² region $15^\circ < \theta < 164^\circ$. The transverse-momentum resolution for full-length tracks is $\sigma(p_T)/p_T = 0.0058p_T \oplus 0.0065 \oplus 0.0014/p_T$, with p_T in GeV. To estimate the energy loss per unit length, dE/dx , of particles in the CTD [15], the truncated mean of the anode-wire pulse heights was calculated, which removes the lowest 10% and at least the highest 30% depending on the number of saturated hits. The measured dE/dx values were corrected by normalising to the dE/dx peak position for tracks around the region of minimum ionisation for pions, $0.3 < p < 0.4$ GeV. Henceforth dE/dx is quoted in units of minimum ionising particles (mips). The resolution of the dE/dx measurement for full-length tracks is about 9%.

The high-resolution uranium–scintillator calorimeter (CAL) [16] consists of three parts: the forward (FCAL), the barrel (BCAL) and the rear (RCAL) calorimeters. Each part is subdivided transversely into towers and longitudinally into one electromagnetic section (EMC) and either one (in RCAL) or two (in BCAL and FCAL) hadronic sections (HAC). The smallest subdivision of the calorimeter is called a cell. The CAL energy resolutions, as measured under test-beam conditions, are $\sigma(E)/E = 0.18/\sqrt{E}$ for electrons and $\sigma(E)/E = 0.35/\sqrt{E}$ for hadrons, with E in GeV. The position of electrons scattered with a small angle with respect to the electron beam direction was measured using the small-angle rear tracking detector (SRTD) [17].

The luminosity was determined from the rate of the bremsstrahlung process $ep \rightarrow e\gamma p$, where the photon was measured with a lead–scintillator calorimeter [18] located at $Z = -107$ m.

3 Event simulation

Monte Carlo (MC) samples of charm and beauty events were produced with the PYTHIA 6.156 [19] and RAPGAP 2.0818 [20] event generators. The generation included direct photon processes, in which the photon couples directly to a parton in the proton, and resolved photon processes, where the photon acts as a source of partons, one of which participates

² The ZEUS coordinate system is a right-handed Cartesian system, with the Z axis pointing in the proton beam direction, referred to as the “forward direction”, and the X axis pointing left towards the centre of HERA. The coordinate origin is at the nominal interaction point.

in the hard scattering process. The CTEQ5L [21] and GRV LO [22] parameterisations were used for the proton and photon structure functions, respectively. The Lund string model [23] as implemented in JETSET [19] was used for hadronisation. The Bowler modification [24] of the LUND symmetric fragmentation function [25] was used for the charm and bottom quark fragmentation. The charm and bottom quark masses were set to the values 1.5 GeV and 4.75 GeV, respectively. All processes were generated in proportion to the predicted MC cross sections. The combined sample of the PYTHIA events, generated with $Q^2 < 0.6 \text{ GeV}^2$, and the RAPGAP events, generated with $Q^2 > 0.6 \text{ GeV}^2$, was used as the inclusive $D^{*\pm}$ MC sample after reweighting the $D^{*\pm}$ transverse momentum, $p_T(D^{*\pm})$, and pseudorapidity, $\eta(D^{*\pm})$, distributions to describe the data.

To generate the Θ_c^0 , the mass of a neutral charmed baryon in the JETSET particle table was set to 3.099 GeV [12], its width was set to zero and the decay channel was set to $D^{*-}p$. The Θ_c^0 samples produced with the PYTHIA and RAPGAP generators were combined in the same way as described in the previous paragraph. Since the production mechanism of the Θ_c^0 is unknown, the simulated $p_T(\Theta_c^0)$ and $\eta(\Theta_c^0)$ distributions were reweighted to the $p_T(D^{*\pm})$ and $\eta(D^{*\pm})$ distributions of the inclusive $D^{*\pm}$ MC which describes the data.

The generated events were passed through a full simulation of the detector using GEANT 3.13 [26] and processed with the same reconstruction program as used for the data.

4 Event selection and reconstruction of $D^{*\pm}$ mesons

The $D^{*\pm}(2010)$ mesons were identified using the two decay channels

$$D^{*+} \rightarrow D^0 \pi_s^+ \rightarrow (K^- \pi^+) \pi_s^+, \quad (1)$$

$$D^{*+} \rightarrow D^0 \pi_s^+ \rightarrow (K^- \pi^+ \pi^+ \pi^-) \pi_s^+. \quad (2)$$

Charge-conjugate processes are included. The π_s particle from the $D^{*\pm}$ decay is referred to as the “soft pion” because it is constrained to have limited momentum by the small mass difference between the D^{*+} and D^0 .

Events from both photoproduction [27] and DIS [28] were selected online with a three-level trigger [13,29]. At the third level, where the full event information was available, the nominal D^* trigger branch required the presence of a reconstructed D^* -meson candidate and, for DIS, a scattered-electron candidate. The efficiency of the online D^* reconstruction, determined relative to the efficiency of the offline D^* reconstruction using an inclusive DIS trigger and a photoproduction dijet trigger, was above 95% for most of the data-taking

period. Events missed by the nominal D^* trigger but selected with some other trigger branch were also used in this analysis.

In the offline analysis, only events with $|Z_{\text{vertex}}| < 50\text{ cm}$, where Z_{vertex} is the primary vertex position determined from the CTD tracks, were used. For each event, a search for the scattered electron from the pattern of energy deposits in the CAL [30] was performed. If a scattered-electron candidate was found, the following criteria were imposed to select DIS events:

- the scattered electron energy above 8 GeV;
- the impact point of the scattered electron on the RCAL outside the (X, Y) region (24cm, 12cm) centered on the beamline;
- $40 < E - P_Z < 65\text{ GeV}$, where $E - P_Z = \sum_i (E - P_Z)_i$ and the sum runs over a combination of charged tracks, as measured in the CTD, and energy clusters measured in the CAL [31];
- $y < 0.95$, where y is the fraction of the electron energy transferred to the proton in its rest frame. For this cut, y was calculated from the energy and angle of the scattered electron;
- $Q^2 > 1\text{ GeV}^2$, using measurements of the energy and angle of the scattered electron.

All events which failed the DIS selection were assigned to the photoproduction sample. Monte Carlo studies showed that 98% of the DIS sample consisted of events with true $Q^2 > 1\text{ GeV}^2$ and 95% of the photoproduction sample consisted of events with true $Q^2 < 1\text{ GeV}^2$. The migrations were taken into account in the correction procedure for detector effects (Section 7).

In each event, charged tracks measured by the CTD and assigned to the primary event vertex were selected. The transverse momentum was required to be greater than 0.1 GeV. Each track was required to reach at least the third superlayer of the CTD. These restrictions ensured both good track acceptance and good momentum resolution.

Selected tracks were combined to form D^0 candidates assuming the decay channels (1) or (2). For both cases, D^0 candidates were formed by calculating the invariant mass $M(K\pi)$ or $M(K\pi\pi\pi)$ for combinations having a total charge of zero. The soft pion was required to have a charge opposite to that of the particle taken as a kaon and was used to form a D^* candidate having mass $M(K\pi\pi_s)$ or $M(K\pi\pi\pi\pi_s)$. No particle identification was used, so kaon and pion masses were assigned in turn to each track.

To reduce the combinatorial background, the following transverse momentum requirements were applied to tracks from the above combinations:

$$p_T(K) > 0.45\text{ GeV}, \quad p_T(\pi) > 0.45\text{ GeV}, \quad p_T(\pi_s) > 0.1\text{ GeV}$$

for channel (1), and

$$p_T(K) > 0.5 \text{ GeV}, p_T(\pi) > 0.2 \text{ GeV}, p_T(\pi_s) > 0.15 \text{ GeV}$$

for channel (2). The D^* candidates were required to have $-1.6 < \eta(D^*) < 1.6$, where the CTD acceptance is high. Also, $p_T(D^*) > 1.35 \text{ GeV}$ or $p_T(D^*) > 2.8 \text{ GeV}$ for channels (1) or (2), respectively, was required to further reduce the combinatorial background.

For selected D^* candidates, consistency of the $M(K\pi)$ or $M(K\pi\pi\pi)$ value with the nominal D^0 mass was required. To take account of the mass resolution, the requirement was

$$1.83 < M(K\pi) < 1.90 \text{ GeV}, 1.845 < M(K\pi\pi\pi) < 1.885 \text{ GeV}$$

for $p_T(D^*) < 5 \text{ GeV}$,

$$1.82 < M(K\pi) < 1.91 \text{ GeV}, 1.835 < M(K\pi\pi\pi) < 1.895 \text{ GeV}$$

for $5 < p_T(D^*) < 8 \text{ GeV}$, and

$$1.81 < M(K\pi) < 1.92 \text{ GeV}, 1.825 < M(K\pi\pi\pi) < 1.905 \text{ GeV}$$

for $p_T(D^*) > 8 \text{ GeV}$.

To suppress the combinatorial background, a cut on the ratio $p_T(D^*)/E_T^{\theta>10}$ was applied, where $E_T^{\theta>10}$ is the transverse energy measured in the CAL outside a cone of $\theta = 10^\circ$ around the forward direction. For DIS events, the energy assigned to the scattered electron was excluded from the $E_T^{\theta>10}$ calculation. The cut value was $p_T(D^*)/E_T^{\theta>10} > 0.12$ and $p_T(D^*)/E_T^{\theta>10} > 0.2$ for channels (1) and (2), respectively. Monte Carlo studies showed that this cut removed a significant fraction of the background whilst preserving most of the D^* mesons produced either inclusively or in Θ_c^0 decays.

The mass difference $\Delta M = M(K\pi\pi_s) - M(K\pi)$ for channel (1) or $\Delta M = M(K\pi\pi\pi\pi_s) - M(K\pi\pi\pi)$ for channel (2) was evaluated for all remaining D^* candidates. Figures 1a and 1b show the mass-difference distributions for channels (1) and (2), respectively. In Figs. 1c and 1d, the mass-difference distributions are shown for DIS events with $Q^2 > 1 \text{ GeV}^2$. Peaks at the nominal value of $M(D^{*+}) - M(D^0)$ are evident. For channel (2), the same tracks can produce two D^0 candidates due to an ambiguity in the kaon and pion mass assignment to tracks with the same charge. Such candidates produce different $M(K\pi\pi\pi)$ values and almost identical ΔM values. To exclude double counting, both combinations of the same tracks which passed all cuts, including the $M(K\pi\pi\pi)$ requirement, were included with a weight 1/2.

To determine the background under the peak, wrong-charge combinations were used. For both channels (1) and (2), these are defined as combinations with total charge ± 2 for the

D^0 candidate and total charge ± 1 for the D^* candidate. The histograms in Fig. 1 show the ΔM distributions for the wrong-charge combinations, normalised to the distributions of D^* candidates with the appropriate charges in the range $0.15 < \Delta M < 0.17$ GeV for channel (1) and $0.15 < \Delta M < 0.16$ GeV for channel (2). The upper ends of the normalisation ranges correspond to the trigger selections of D^* candidates in the two decay channels. For both channels, the same tracks from a wrong-charge combination can produce two D^0 candidates due to an ambiguity in the kaon and pion mass assignment to tracks with the same charge. For channel (2), it is also possible to have three wrong-charge D^0 candidates produced by the same tracks. To exclude double and triple counting, the multiple combinations of the same tracks which passed all cuts, including the $M(K\pi)$ or $M(K\pi\pi\pi)$ requirement, were included with a weight 1/2 or 1/3 for double or triple entries, respectively. Monte Carlo studies showed that the procedure used for the background determination and the treatment of multiple entries permits the recovery of the number of true D^* mesons for both channels (1) and (2).

To improve the signal-to-background ratio, only D^* candidates with $0.144 < \Delta M < 0.147$ GeV for channel (1) and $0.1445 < \Delta M < 0.1465$ GeV for channel (2) were kept for the charmed pentaquark search. After background subtraction, signals of 42680 ± 350 $D^{*\pm}$ mesons in channel (1) and 19900 ± 250 D^* mesons in channel (2) were found in the above ΔM ranges. In DIS with $Q^2 > 1$ GeV², the numbers of reconstructed D^* mesons were 8680 ± 130 in channel (1) and 4830 ± 120 in channel (2), whereas for $Q^2 < 1$ GeV² 34000 ± 330 and 15070 ± 220 D^* mesons were found in channels (1) and (2), respectively.

The relative acceptance for D^* mesons originating from the Θ_c^0 and D^* mesons produced inclusively, $A^{\Theta_c^0}(D^*)/A^{\text{inc}}(D^*)$, was calculated using the Θ_c^0 and the inclusive D^* MC samples. The values of this relative acceptance were 85% and 87% for the samples with D^* reconstructed in the decay channels (1) and (2), respectively.

5 Selection of proton candidates and D^*p invariant mass reconstruction

A charmed pentaquark candidate was formed by combining a selected D^* candidate with a track, assumed to be a proton, with $p_T > 0.15$ GeV and a charge opposite to that of the D^* . For each charmed pentaquark candidate, the “extended” mass difference, $\Delta M^{\text{ext}} = M(K\pi\pi_s p) - M(K\pi\pi_s)$ or $\Delta M^{\text{ext}} = M(K\pi\pi\pi_s p) - M(K\pi\pi\pi_s)$, was calculated. The invariant mass of the D^*p system was calculated as $M(D^*p) = \Delta M^{\text{ext}} + M(D^{*+})_{\text{PDG}}$, where $M(D^{*+})_{\text{PDG}}$ is the nominal $D^{*\pm}$ mass [32]. The resolution in $M(D^*p)$ for $M(D^*p) \sim 3.1$ GeV, where a narrow signal was reported by the H1 Collaboration [12], was estimated from MC simulations to be 4 MeV.

To reduce pion and kaon backgrounds, the measured dE/dx values for proton candidates were used. To ensure good dE/dx resolution, at least eight CTD hits were used. Figure 2 shows the dE/dx values as a function of momentum, P , for particles which yield a mass $M(D^*p) < 3.6$ GeV. The proton bands are clearly seen in the distributions for particles associated with D^* in both decay channels. The parameterisation for the expectation value of dE/dx as a function of P/m was obtained using tagged protons from Λ^0 decays and tagged pions from K_s^0 decays. To construct a χ_1^2 function, the following procedure [33] was used. For each particle, a χ_1^2 value that estimates the deviation of the measured dE/dx from the expectation was calculated as:

$$\chi_1^2 = \frac{[\ln(dE/dx) - \ln(dE/dx)_{\text{expected}}]^2}{\sigma_{\ln(dE/dx)}^2}.$$

The resolution was parameterised empirically as $\sigma_{\ln(dE/dx)} = a/\sqrt{n}$, where n is the number of hits used for the dE/dx measurement and a is a constant determined from the sample of tagged protons. The χ_1^2 probability of the proton hypothesis, l_p , is given by the probability for a proton to produce the observed or a larger value of χ_1^2 .

The distribution of l_p for proton candidates shows a sharp peak at $l_p \sim 0$ and becomes relatively flat towards $l_p \sim 1$. To maximise the ratio of the number of selected protons to the square root of the number of background particles, a cut $l_p > 0.15$ was applied.

The acceptance of the proton selection before the requirement on l_p , $A(p)$, was calculated using the Θ_c^0 MC to be 85% and 89% for the samples with D^* reconstructed in the decay channels (1) and (2), respectively. The acceptance $A(l_p > 0.15)$ was calculated, using the tagged protons, to be $(85.0 \pm 0.1)\%$. This acceptance, calculated directly from the data, was insensitive to the proton momenta spectrum.

6 D^*p invariant mass distributions

Figure 3a shows the $M(D^*p)$ distribution³ for D^* meson candidates reconstructed in the decay channel (1). No narrow resonance is seen. To suppress the large background from pion and kaon tracks, the following two selections were used in addition to the general proton selection described in Section 5:

- low-momentum selection: only tracks with $P < 1.35$ GeV and $dE/dx > 1.3$ mips were used as proton candidates. These requirements select clean proton samples corresponding to the proton bands separated from the pion and kaon bands in Fig. 2;

³ The $M(D^*p)$ distributions, shown in this paper for $M(D^*p) < 3.6$ GeV, were investigated in the full kinematically allowed range.

- high-momentum selection: only tracks with $P > 2 \text{ GeV}$ were used as proton candidates. This selection was suggested by the observation of the H1 Collaboration [12] that the signal-to-background ratio for charmed pentaquarks improves as the proton momentum increases.

Figures 3b and 3c show the $M(D^*p)$ distributions for the low-momentum and high-momentum proton selections, respectively. The selections reveal no narrow resonance.

Figure 4a shows the $M(D^*p)$ distribution, obtained with D^* meson candidates reconstructed in the decay channel (1), for DIS with $Q^2 > 1 \text{ GeV}^2$. Figures 4b and 4c show the $M(D^*p)$ distributions for the low-momentum and high-momentum proton selections, respectively. No narrow resonance is seen in either distribution.

Figure 5 shows the $M(D^*p)$ distributions, obtained with D^* meson candidates reconstructed in the decay channel (2), for the full data sample (Fig. 5a) and for DIS with $Q^2 > 1 \text{ GeV}^2$ (Fig. 5b). Both distributions show no narrow resonance. No resonance was also observed using the low-momentum and high-momentum proton selections with D^* meson candidates reconstructed in the decay channel (2) (not shown).

The histograms in Figs. 3-5 show the $M(D^*p)$ distributions for like-sign combinations of $D^{*\pm}$ and proton candidates. The shapes of the mass distributions for the unlike-sign and like-sign combinations are similar. The like-sign distributions lie below the unlike-sign distributions at low $M(D^*p)$ values, which is consistent with MC predictions.

6.1 Systematic checks

The selection cuts were varied to check that the pentaquark signal was not lost due to some specific selection requirement or hidden by the combinatorial background. In particular, the following systematic checks were carried out:

- variations were made in the cuts on l_p and on the number of CTD hits used for the dE/dx measurement;
- the cut on l_p was replaced by a requirement for proton candidate tracks to lie within a wide dE/dx band [4];
- the high-momentum proton selection was repeated without cuts on l_p or on the number of CTD hits used for the dE/dx measurement;
- to reduce the pion background in the proton candidate sample, reflections from the decays of the excited D mesons, $D_1^0, D_2^{*0} \rightarrow D^{*\pm} \pi^\mp$, to the $M(D^{*\pm} p^\mp)$ spectra were removed by excluding all combinations with $2.38 < M(D^{*\pm} \pi^\mp) < 2.5 \text{ GeV}$;
- DIS events were selected with $Q^2 > 20 \text{ GeV}^2$, i.e. in the range where the cleanest Θ^+ signal was observed in the previous ZEUS analysis [4]. Using this selection, the

numbers of reconstructed D^* mesons were 2326 ± 67 in channel (1) and 1799 ± 78 in channel (2);

- DIS events were selected using only the inclusive DIS trigger. Using this selection, the numbers of reconstructed D^* mesons were 3426 ± 82 in channel (1) and 2369 ± 86 in channel (2);
- tracks not assigned to the primary event vertex were used together with the primary vertex tracks for D^* reconstruction and proton candidate selection.

No signal was observed using any of these selection variations.

The analysis was also repeated for the D^* decay channel (1) using very similar selection criteria used in the analysis of the H1 collaboration [12]. The minimum transverse momentum requirements applied to tracks forming D^* combinations were set to the H1 values. The cut $p_T(D^*)/E_T^{\theta > 10} > 0.12$ used in the ZEUS analysis was replaced by the cut $z(D^*) > 0.2$, where $z(D^*) = P \cdot p(D^*)/P \cdot q$ and P , $p(D^*)$ and q are the four-momenta of the incoming proton, the D^* meson and the exchanged photon. In the proton rest frame, $z(D^*)$ is the fraction of the photon energy carried by the $D^{*\pm}$ meson. The requirements on $M(K\pi)$ and ΔM were kept as in the nominal ZEUS analysis since they were determined by the mass resolution of the ZEUS CTD.⁴ The DIS events were selected with $Q^2 > 1 \text{ GeV}^2$ and $0.05 < y < 0.7$, while the photoproduction events were selected with $Q^2 < 1 \text{ GeV}^2$ and $0.2 < y < 0.8$. The D^* candidates were required to have $-1.5 < \eta(D^*) < 1.0$ and $p_T(D^*) > 1.5 \text{ GeV}$ or $p_T(D^*) > 2.0 \text{ GeV}$ in DIS or photoproduction selections, respectively. The numbers of reconstructed D^* mesons found using these cuts were 5920 ± 90 and 11670 ± 140 for the DIS and photoproduction selections, respectively. To select proton candidates, the requirement $l_p > 0.15$ was replaced by the H1 requirements on the normalised proton likelihood [12]. The range of the proton momentum $1.6 - 2.0 \text{ GeV}$ was excluded in the case of photoproduction.

Figure 6 shows the $M(D^*p)$ distributions separately for the DIS and photoproduction events selected using the H1 criteria. There is no indication of a narrow resonance in either distribution. Yields of combinations in the ZEUS and H1 $M(D^*p)$ distributions for DIS are in approximate proportion to the corresponding numbers of D^* mesons. The histograms in Fig. 6 show a two-component model in which the wrong charge $(K\pi)\pi_s$ combinations, normalised as described in Section 4, were used to describe the non-charm contribution, and the inclusive D^* MC simulation, normalised to the D^* yield in the data, described the contribution of real D^* mesons. The model describes the measured $M(D^*p)$ distributions well.

⁴ The check was also repeated with the H1 requirements on $M(K\pi)$ and ΔM .

7 Evaluation of upper limits

Upper limits on the fraction of D^* mesons originating from the Θ_c^0 decays were set in the signal window $3.07 < M(D^*p) < 3.13$ GeV. This window covers the H1 measurement taking into account the uncertainties of the measured Θ_c^0 mass and width. The upper limits were calculated for the full D^* -meson samples obtained with D^* reconstructed in channels (1) and (2), see Figs. 7a and 7b. The calculations were also separately repeated with the samples obtained in DIS (see Figs. 7c and 7d) and photoproduction (not shown). Each $M(D^*p)$ distribution was fitted outside the signal window to the functional form $x^a \exp(-bx + cx^2)$, where $x = \Delta M^{\text{ext}} - m_p$ and m_p is the proton mass. The fitted curves describe the $M(D^*p)$ distributions reasonably well in the whole range shown in Fig. 7. The number of reconstructed Θ_c^0 baryons was estimated by subtracting the background function, integrated over the signal window, from the observed number of candidates in the window. This number was divided by the number of reconstructed D^* mesons, yielding the fraction of D^* mesons originating from the Θ_c^0 decays, $R(\Theta_c^0 \rightarrow D^*p/D^*)$.

The numbers used for the upper-limit calculations and the measured upper limits are summarised in Table 1. The reported upper limits are the frequentist confidence bounds calculated assuming a Gaussian probability function in the unified approach [34]. The results are shown separately for the full data sample, for DIS with $Q^2 > 1 \text{ GeV}^2$ and for photoproduction with $Q^2 < 1 \text{ GeV}^2$.

The 95% C.L. upper limits on $R(\Theta_c^0 \rightarrow D^*p/D^*)$ were found to be 0.29% and 0.33% for the full D^* -meson samples obtained with D^* reconstructed in channels (1) and (2), respectively. To average the $R(\Theta_c^0 \rightarrow D^*p/D^*)$ values obtained with D^* reconstructed in the two decay channels, a standard weighted least-square procedure [32] was used. The combined upper limit from both decay channels is 0.23%. The combined upper limit for DIS with $Q^2 > 1 \text{ GeV}^2$ is 0.35%.

The H1 Collaboration reported a Θ_c^0 baryon contributing roughly 1% of the D^* production rate, in the kinematic region studied in that analysis, in DIS with $Q^2 > 1 \text{ GeV}^2$, and a clear signal of compatible mass and width in a photoproduction sample ($Q^2 < 1 \text{ GeV}^2$) [12]. If the Θ_c^0 baryon contributed 1% of the number of D^* mesons in the kinematic region studied in this analysis, a signal of 626 Θ_c^0 baryons would be expected using the full samples of the D^* mesons reconstructed in both decay channels. Assuming Gaussian statistics, such a signal together with the expected number of background events could produce the observed number of events in the signal window only in cases of statistical fluctuations larger than 9σ . A production rate corresponding to 1% of D^* 's of the present analysis in the DIS ($Q^2 > 1 \text{ GeV}^2$) sample only is excluded at 5σ . In Fig. 7, the MC Θ_c^0 signals normalised to 1% of the numbers of reconstructed D^* mesons are shown on top of the fitted backgrounds.

To correct the fraction of D^* mesons originating from the Θ_c^0 decays for detector effects, the relative acceptance was calculated from the acceptances defined in Sections 4 and 5 as:

$$\frac{A(\Theta_c^0 \rightarrow D^* p)}{A^{\text{inc}}(D^*)} = \frac{A^{\Theta_c^0}(D^*)}{A^{\text{inc}}(D^*)} \cdot A(p) \cdot A(l_p > 0.15).$$

The systematic uncertainty of the background fit procedure was estimated by varying the range used in the fit. To estimate the systematic uncertainty in the MC correction factors, the $p_T(\Theta_c^0)$ and $\eta(\Theta_c^0)$ spectra of the Θ_c^0 MC were varied. Both systematic uncertainties and the statistical uncertainties of the data, MC and $A(l_p > 0.15)$ were added in quadrature to determine the total uncertainty used for the upper-limit calculation. The 95% C.L. upper limits on the corrected fraction of D^* mesons originating from Θ_c^0 decays, $R^{\text{cor}}(\Theta_c^0 \rightarrow D^* p / D^*)$, were found to be 0.47% and 0.50% for the full D^* -meson samples obtained with D^* reconstructed in channels (1) and (2), respectively. The combined upper limit from both decay channels is 0.37%. The effect of correlated systematic uncertainties was negligible in the combined upper limit calculation.

The product of the fraction of c quarks hadronising as a Θ_c^0 baryon, $f(c \rightarrow \Theta_c^0)$, and the branching ratio of the Θ_c^0 decay to $D^* p$, $B_{\Theta_c^0 \rightarrow D^* p}$, can be calculated as:

$$f(c \rightarrow \Theta_c^0) \cdot B_{\Theta_c^0 \rightarrow D^* p} = \frac{N(\Theta_c^0 \rightarrow D^* p)}{N(D^*)} \cdot f(c \rightarrow D^{*+}),$$

where $f(c \rightarrow D^{*+})$ is the known rate of c quarks hadronising as D^{*+} mesons [35] and the ratio of the numbers of the Θ_c^0 and D^* hadrons, $\frac{N(\Theta_c^0 \rightarrow D^* p)}{N(D^*)}$, is calculated in the full phase space. An extrapolation of the fractions measured in the restricted $p_T(D^*)$ and $\eta(D^*)$ kinematic ranges to the full phase space would require precise modelling of the $p_T(\Theta_c^0)$ and $\eta(\Theta_c^0)$ spectra. Such modelling is currently not available. To estimate the upper limit on $f(c \rightarrow \Theta_c^0) \cdot B_{\Theta_c^0 \rightarrow D^* p}$, the corrected fractions of D^* mesons originating from the Θ_c^0 decays were converted to the ratios of numbers of the Θ_c^0 and D^* hadrons in their respective kinematic ranges used for the D^* meson selection:

$$\frac{N(\Theta_c^0 \rightarrow D^* p; p_T(\Theta_c^0) > 1.35, 2.8 \text{ GeV}; |\eta(\Theta_c^0)| < 1.6)}{N(D^*; p_T(D^*) > 1.35, 2.8 \text{ GeV}; |\eta(D^*)| < 1.6)} = R^{\text{cor}}(\Theta_c^0 \rightarrow D^* p / D^*) \cdot f^{\text{conv}},$$

$$f^{\text{conv}} = \frac{N(\Theta_c^0 \rightarrow D^* p; p_T(\Theta_c^0) > 1.35, 2.8 \text{ GeV}; |\eta(\Theta_c^0)| < 1.6)}{N(\Theta_c^0 \rightarrow D^* p; p_T(D^*) > 1.35, 2.8 \text{ GeV}; |\eta(D^*)| < 1.6)}.$$

The conversion factors, f^{conv} , obtained with the Θ_c^0 MC, were 1.6 and 2.8 for $p_T > 1.35 \text{ GeV}$ and $p_T > 2.8 \text{ GeV}$, respectively. Using these conversion factors, the 95% C.L. upper limits on $f(c \rightarrow \Theta_c^0) \cdot B_{\Theta_c^0 \rightarrow D^* p}$, were estimated to be 0.18% and 0.33% for the full D^* -meson samples obtained with D^* reconstructed in channels (1) and (2), respectively. The combined upper limit from both decay channels is 0.16%. The effect of correlated systematic uncertainties was negligible in the combined upper limit calculation.

8 Summary

A resonance search has been made in the $D^{*\pm}p^\mp$ invariant-mass spectrum with the ZEUS detector at HERA using an integrated luminosity of 126 pb^{-1} . The decay channels $D^{*+} \rightarrow D^0\pi_s^+ \rightarrow (K^-\pi^+)\pi_s^+$ and $D^{*+} \rightarrow D^0\pi_s^+ \rightarrow (K^-\pi^+\pi^+\pi^-)\pi_s^+$ (and the corresponding antiparticle decays) were used to identify $D^{*\pm}$ mesons. No resonance structure was observed in the $M(D^{*\pm}p^\mp)$ spectrum from more than 60 000 reconstructed $D^{*\pm}$ mesons. The upper limit on the fraction of D^* mesons originating from Θ_c^0 decays is 0.23% (95% C.L.). The upper limit for DIS with $Q^2 > 1\text{ GeV}^2$ is 0.35% (95% C.L.). Thus, the ZEUS data are not compatible with the H1 report of Θ_c^0 baryon production in DIS and photoproduction, with a rate, in DIS, of roughly 1% of the D^* production rate.

9 Acknowledgements

We would like to thank the DESY Directorate for their strong support and encouragement. The remarkable achievements of the HERA machine group were vital for the successful completion of this work and are greatly appreciated. We thank Marek Karliner, Harry Lipkin and Torbjörn Sjöstrand for useful discussions.

References

- [1] LEPS Collab., T. Nakano et al., Phys. Rev. Lett. **91**, 012002 (2003);
DIANA Collab., V.V. Barmin et al., Phys. Atom. Nucl. **66**, 1715 (2003);
CLAS Collab., S. Stepanyan et al., Phys. Lett. **91**, 252001 (2003);
SAPHIR Collab., J. Barth et al., Phys. Lett. **B 572**, 123 (2003);
A.E. Asratyan, A.G. Dolgolenko and M.A. Kubantsev, Phys. Atom. Nucl. **67**, 682 (2004);
CLAS Collab., V. Kubarovsky et al., Phys. Rev. Lett. **92**, 032001 (2004).
Erratum-ibid **92**, 049902 (2004);
HERMES Collab., A. Airapetian et al., Phys. Lett. **B 585**, 213 (2004);
SVD Collab., A. Aleev et al., Preprint hep-ex/0401024, (2004). Subm. to Phys. Atom. Nucl;
COSY-TOF Collab., M. Abdel-Bary et al., Phys. Lett. **B 595**, 127 (2004).
- [2] NA49 Collab., C. Alt et al., Phys. Rev. Lett. **92**, 042003 (2004).
- [3] BES Collab., J.Z. Bai et al., Phys. Rev. **D 70**, 012004 (2004);
HERA-B Collab., I. Abt et al., Preprint hep-ex/0408048, (2004).
- [4] ZEUS Collab., S. Chekanov et al., Phys. Lett. **B 591**, 7 (2004).
- [5] D. Diakonov, V. Petrov and M.V. Polyakov, Z. Phys. **A 359**, 305 (1997).
- [6] R.L. Jaffe and F. Wilczek, Phys. Rev. Lett. **91**, 232003 (2003).
- [7] H. Walliser and B. Kopeliovich, J. Exp. Theor. Phys. **97**, 433 (2003);
S. Capstick, P.R. Page and W. Roberts, Phys. Lett. **B 570**, 185 (2003);
M. Karliner and H. Lipkin, Phys. Lett. **B 575**, 249 (2003).
- [8] C. Cignoux, B. Silvestre-Brac and J. Richard, Phys. Lett. **B 193**, 323 (1987);
H. Lipkin, Phys. Lett. **B 195**, 484 (1987);
D. Riska and N. Scoccola, Phys. Lett. **B 299**, 338 (1993);
F. Stancu, Phys. Rev. **D 58**, 111501 (1998).
- [9] M. Karliner and H. Lipkin, Preprint hep-ph/0307343, 2003.
- [10] K. Cheung, Phys. Rev. **D 69**, 094029 (2004);
B. Wu and B. Ma, Preprint hep-ph/0402244, (2004);
H. Cheng, C. Chua and C. Hwang, Preprint hep-ph/0403232, (2004);
J.J. Dudek, Preprint hep-ph/0403235, (2004).
- [11] M. Karliner. Private communication based on
M. Karliner and H. Lipkin. Phys. Lett. **B 586**, 303 (2004).
- [12] H1 Collab., C. Atkas et al., Phys. Lett. **B 588**, 17 (2004).

- [13] ZEUS Collab., U. Holm (ed.), *The ZEUS Detector*. Status Report (unpublished), DESY (1993), available on <http://www-zeus.desy.de/bluebook/bluebook.html>.
- [14] N. Harnew et al., Nucl. Instr. and Meth. **A 279**, 290 (1989);
B. Foster et al., Nucl. Phys. Proc. Suppl. **B 32**, 181 (1993);
B. Foster et al., Nucl. Instr. and Meth. **A 338**, 254 (1994).
- [15] ZEUS Collab., J. Breitweg et al., Phys. Lett. **B 481**, 213 (2000);
ZEUS Collab., J. Breitweg et al., Eur. Phys. J. **C 18**, 625 (2001).
- [16] M. Derrick et al., Nucl. Instr. and Meth. **A 309**, 77 (1991);
A. Andresen et al., Nucl. Instr. and Meth. **A 309**, 101 (1991);
A. Caldwell et al., Nucl. Instr. and Meth. **A 321**, 356 (1992);
A. Bernstein et al., Nucl. Instr. and Meth. **A 336**, 23 (1993).
- [17] A. Bamberger et al., Nucl. Instr. and Meth. **A 401**, 63 (1997).
- [18] J. Andruszków et al., Preprint DESY-92-066, DESY, 1992;
ZEUS Collab., M. Derrick et al., Z. Phys. **C 63**, 391 (1994);
J. Andruszków et al., Acta Phys. Pol. **B 32**, 2025 (2001).
- [19] T. Sjöstrand, Comp. Phys. Comm. **82**, 74 (1994).
- [20] H. Jung, Comp. Phys. Comm. **86**, 147 (1995).
- [21] CTEQ Collab., H.L. Lai et al., Eur. Phys. J. **C 12**, 375 (2000).
- [22] M. Glück, E. Reya and A. Vogt, Phys. Rev. **D 46**, 1973 (1992).
- [23] B. Andersson et al., Phys. Rep. **97**, 31 (1983).
- [24] M. G. Bowler, Z. Phys. **C 11**, 169 (1981).
- [25] B. Andersson, G. Gustafson and B. Söderberg, Z. Phys. **C 20**, 317 (1983).
- [26] R. Brun et al., GEANT3, Technical Report CERN-DD/EE/84-1, CERN, 1987.
- [27] ZEUS Collab., J. Breitweg et al., Eur. Phys. J. **C 6**, 67 (1999).
- [28] ZEUS Collab., J. Breitweg et al., Eur. Phys. J. **C 12**, 35 (2000);
ZEUS Collab., S. Chekanov et al., Phys. Rev. **D 69**, 0120004 (2004).
- [29] ZEUS Collab., M. Derrick et al., Phys. Lett. **B 293**, 465 (1992).
- [30] H. Abramowicz, A. Caldwell and R. Sinkus, Nucl. Instr. and Meth. **A 365**, 508 (1995).
- [31] G.M. Briskin. Ph.D. Thesis, Tel Aviv University, (1998). (Unpublished).
- [32] Particle Data Group, K. Hagiwara et al., Phys. Rev. **D 66**, 10001 (2002).
- [33] O. Deppe. Ph.D. Thesis, Hamburg University, Report DESY-THESIS-2000-006, (1999).

- [34] G.J. Feldman and R.D. Cousins, Phys. Rev. **D57**, 3873 (1998).
- [35] L. Gladilin, Preprint hep-ex/9912064, (1999).

D^* decay channel	$(K\pi)\pi_s$	$(K\pi\pi\pi)\pi_s$	Both channels
Full data sample			
N_{window}	1710	914	
N_{backgr}	1678 ± 23	919 ± 19	
$N(D^*)$	42680 ± 350	19900 ± 250	
$R(\Theta_c^0 \rightarrow D^*p/D^*)$	$< 0.29\%$	$< 0.33\%$	$< 0.23\%$
$R^{\text{cor}}(\Theta_c^0 \rightarrow D^*p/D^*)$	$< 0.47\%$	$< 0.50\%$	$< 0.37\%$
$f(c \rightarrow \Theta_c^0) \cdot B_{\Theta_c^0 \rightarrow D^*p}$	$< 0.18\%$	$< 0.33\%$	$< 0.16\%$
DIS with $Q^2 > 1 \text{ GeV}^2$			
N_{window}	252	220	
N_{backgr}	252.8 ± 9.2	219.8 ± 8.8	
$N(D^*)$	8680 ± 130	4830 ± 120	
$R(\Theta_c^0 \rightarrow D^*p/D^*)$	$< 0.41\%$	$< 0.69\%$	$< 0.35\%$
$R^{\text{cor}}(\Theta_c^0 \rightarrow D^*p/D^*)$	$< 0.59\%$	$< 1.06\%$	$< 0.51\%$
$f(c \rightarrow \Theta_c^0) \cdot B_{\Theta_c^0 \rightarrow D^*p}$	$< 0.20\%$	$< 0.56\%$	$< 0.19\%$
Photoproduction with $Q^2 < 1 \text{ GeV}^2$			
N_{window}	1458	695	
N_{backgr}	1422 ± 21	694 ± 15	
$N(D^*)$	34000 ± 330	15070 ± 220	
$R(\Theta_c^0 \rightarrow D^*p/D^*)$	$< 0.36\%$	$< 0.40\%$	$< 0.29\%$
$R^{\text{cor}}(\Theta_c^0 \rightarrow D^*p/D^*)$	$< 0.60\%$	$< 0.60\%$	$< 0.47\%$
$f(c \rightarrow \Theta_c^0) \cdot B_{\Theta_c^0 \rightarrow D^*p}$	$< 0.23\%$	$< 0.43\%$	$< 0.21\%$

Table 1: Numbers of the $M(D^*p)$ combinations in the signal window, N_{window} ; fit background estimations, N_{backgr} ; numbers of reconstructed D^* mesons, $N(D^*)$; 95% C.L. upper limits on the uncorrected, $R(\Theta_c^0 \rightarrow D^*p/D^*)$, and corrected, $R^{\text{cor}}(\Theta_c^0 \rightarrow D^*p/D^*)$, fractions of D^* mesons originating from Θ_c^0 decays; and 95% C.L. upper limits on the product of the fraction of c quarks hadronising as a Θ_c^0 baryon, $f(c \rightarrow \Theta_c^0)$, and the branching ratio of the Θ_c^0 decay to D^*p , $B_{\Theta_c^0 \rightarrow D^*p}$. The results are shown for the full data sample, for DIS with $Q^2 > 1 \text{ GeV}^2$ and for photoproduction with $Q^2 < 1 \text{ GeV}^2$.

ZEUS

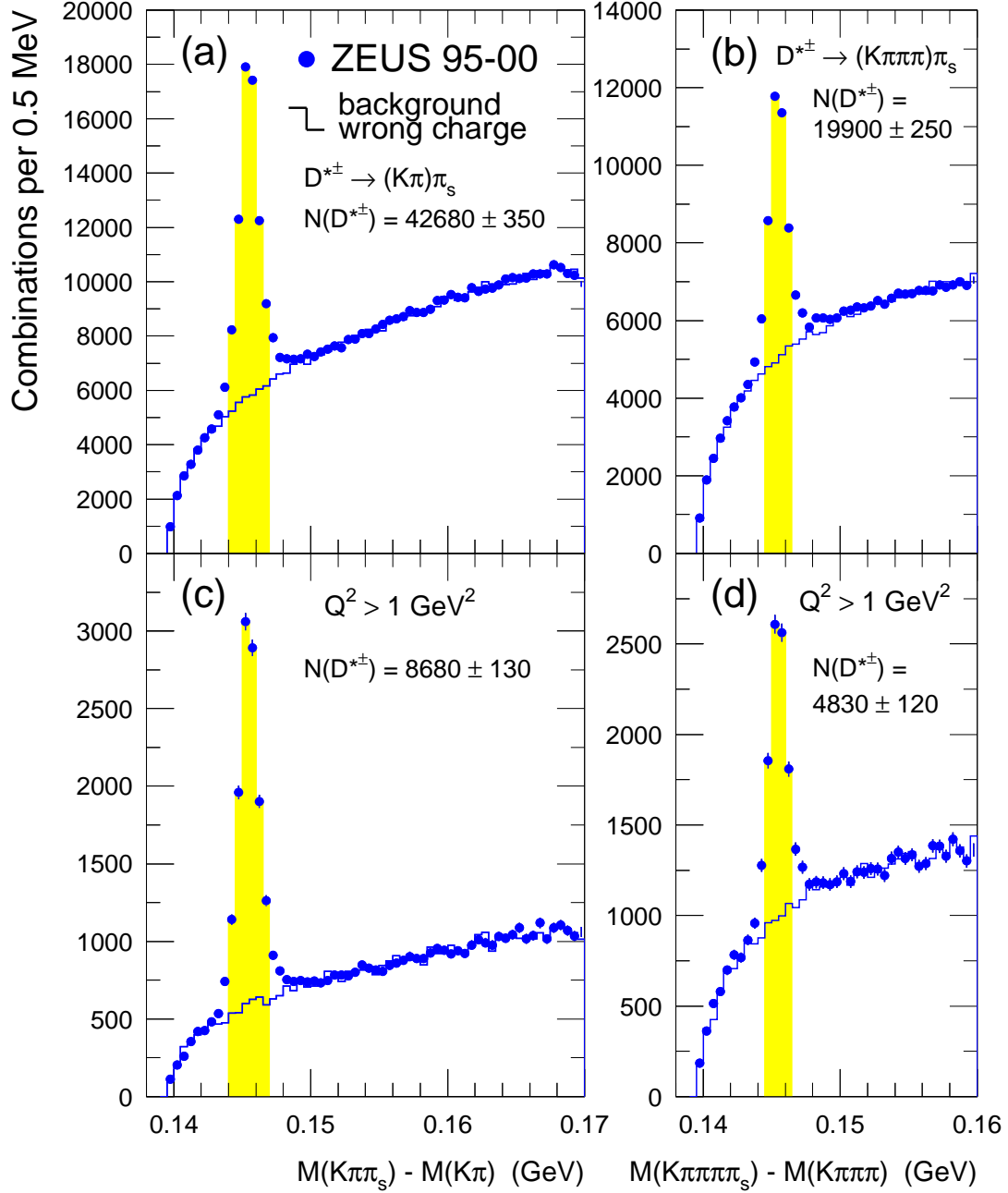


Figure 1: The distribution of the mass difference, ΔM , (dots) for (a) $D^{*\pm} \rightarrow (K\pi)\pi_s$ candidates in the full data sample, (b) $D^{*\pm} \rightarrow (K\pi\pi\pi)\pi_s$ candidates in the full data sample, (c) $D^{*\pm} \rightarrow (K\pi)\pi_s$ candidates in DIS with $Q^2 > 1 \text{ GeV}^2$ and (d) $D^{*\pm} \rightarrow (K\pi\pi\pi)\pi_s$ candidates in DIS with $Q^2 > 1 \text{ GeV}^2$. The histograms show the ΔM distributions for wrong charge combinations. Only $D^{*\pm}$ candidates from the shaded bands were used for the charmed pentaquark search.

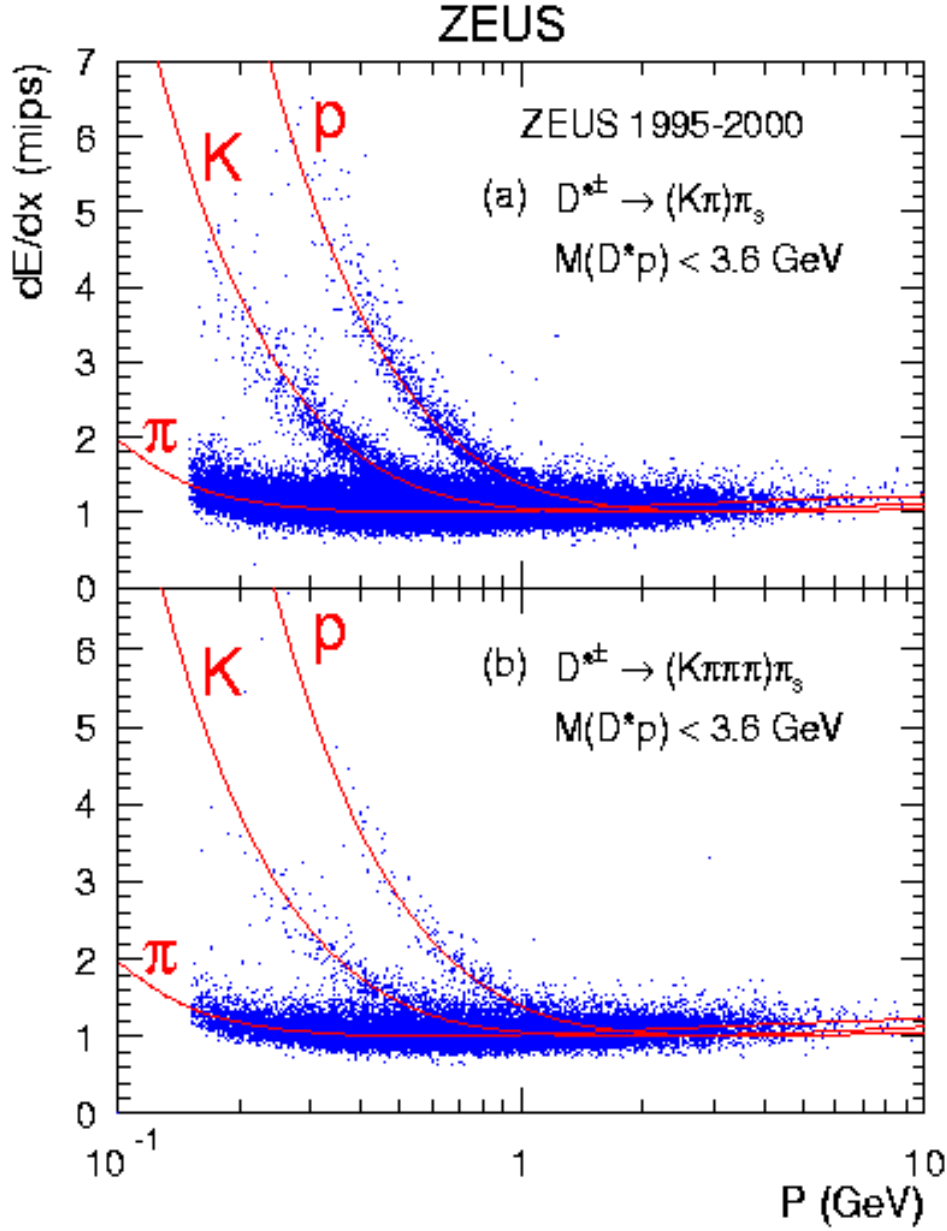


Figure 2: The dE/dx values as a function of momentum, P , for particles which yield a mass $M(D^*p) < 3.6 \text{ GeV}$ when combined with (a) $D^{*\pm} \rightarrow (K\pi)\pi_s$ candidates and (b) $D^{*\pm} \rightarrow (K\pi\pi\pi)\pi_s$ candidates. The lines indicate parameterisations for the expectation values of dE/dx for pions, kaons and protons.

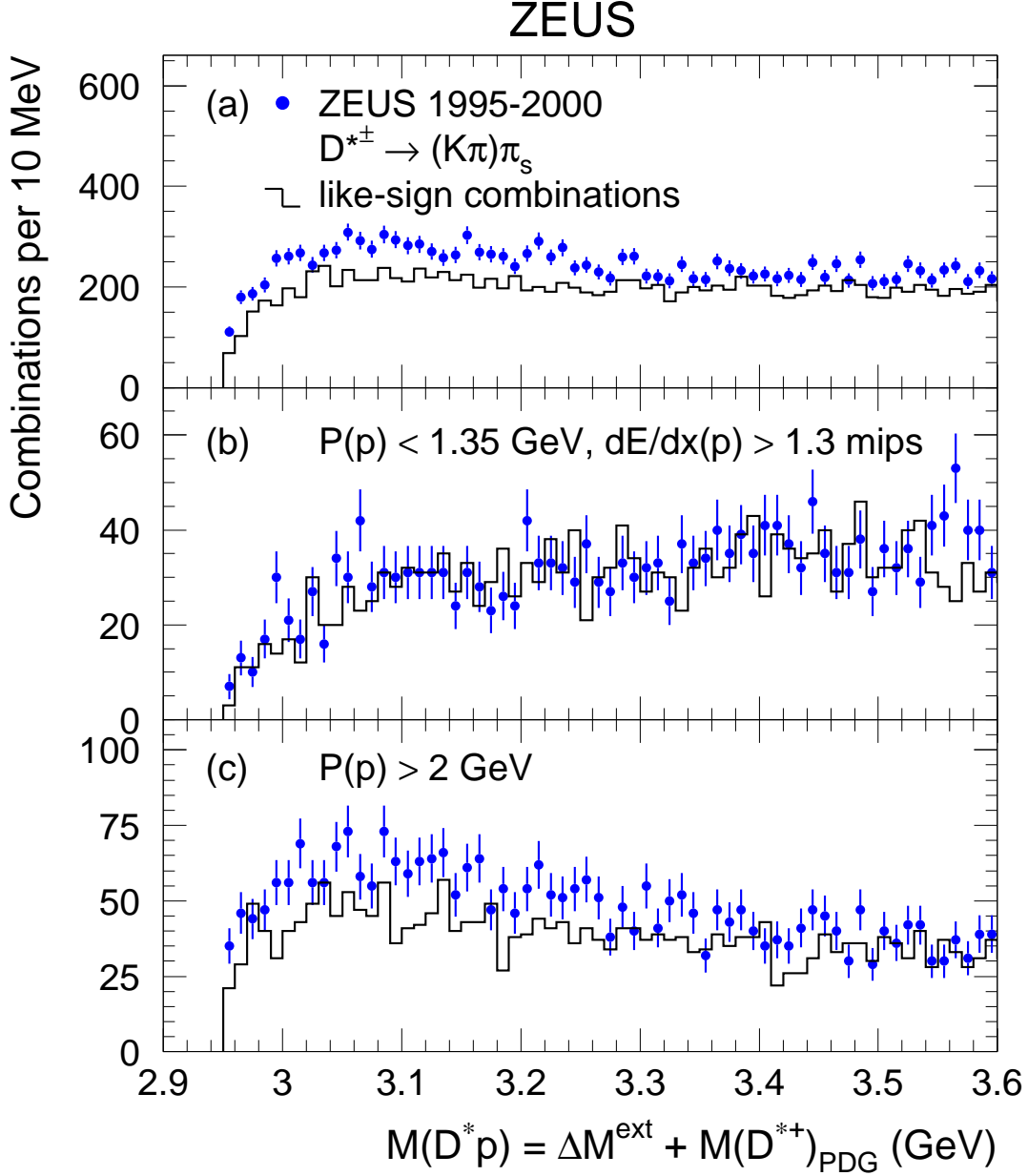


Figure 3: The distribution of $M(D^*p) = \Delta M^{\text{ext}} + M(D^{*+})_{\text{PDG}}$ for charmed pentaquark candidates (dots) obtained with the full data sample using (a) all proton candidates, (b) proton candidates with momentum below 1.35 GeV and dE/dx above 1.3 mips, and (c) proton candidates with momentum above 2 GeV. The extended mass difference is defined as $\Delta M^{\text{ext}} = M(K\pi\pi_s p) - M(K\pi\pi_s)$ and $M(D^{*+})_{\text{PDG}}$ is the nominal D^{*+} mass. The histograms show the $M(D^*p)$ distributions for the like-sign combinations.

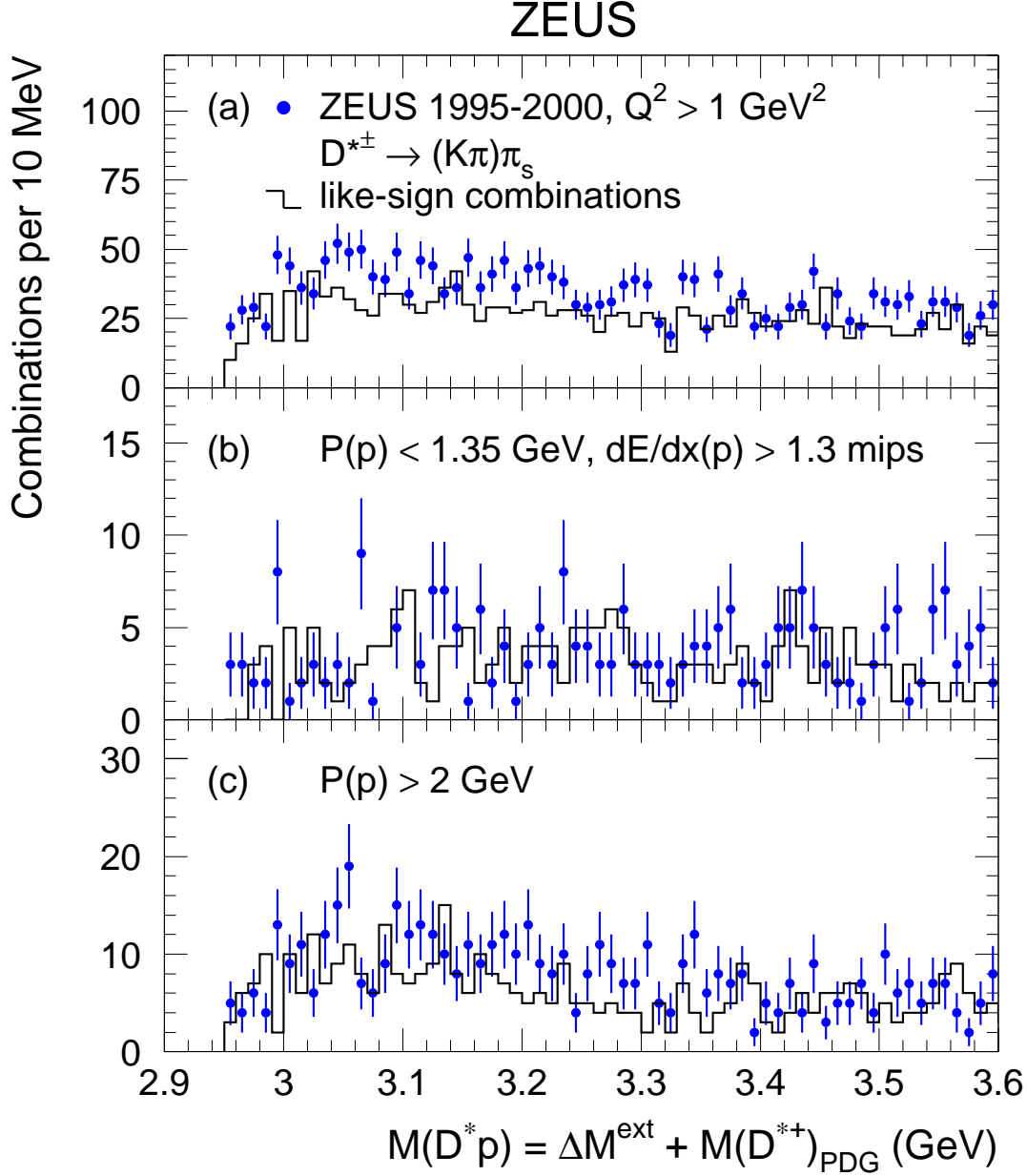


Figure 4: The distribution of $M(D^*p) = \Delta M^{\text{ext}} + M(D^{*+})_{\text{PDG}}$ for charmed pentaquark candidates (dots) obtained in DIS with $Q^2 > 1 \text{ GeV}^2$ using (a) all proton candidates, (b) proton candidates with momentum below 1.35 GeV and dE/dx above 1.3 mips, and (c) proton candidates with momentum above 2 GeV. The extended mass difference is defined as $\Delta M^{\text{ext}} = M(K\pi\pi_s p) - M(K\pi\pi_s)$ and $M(D^{*+})_{\text{PDG}}$ is the nominal D^{*+} mass. The histograms show the $M(D^*p)$ distributions for the like-sign combinations.

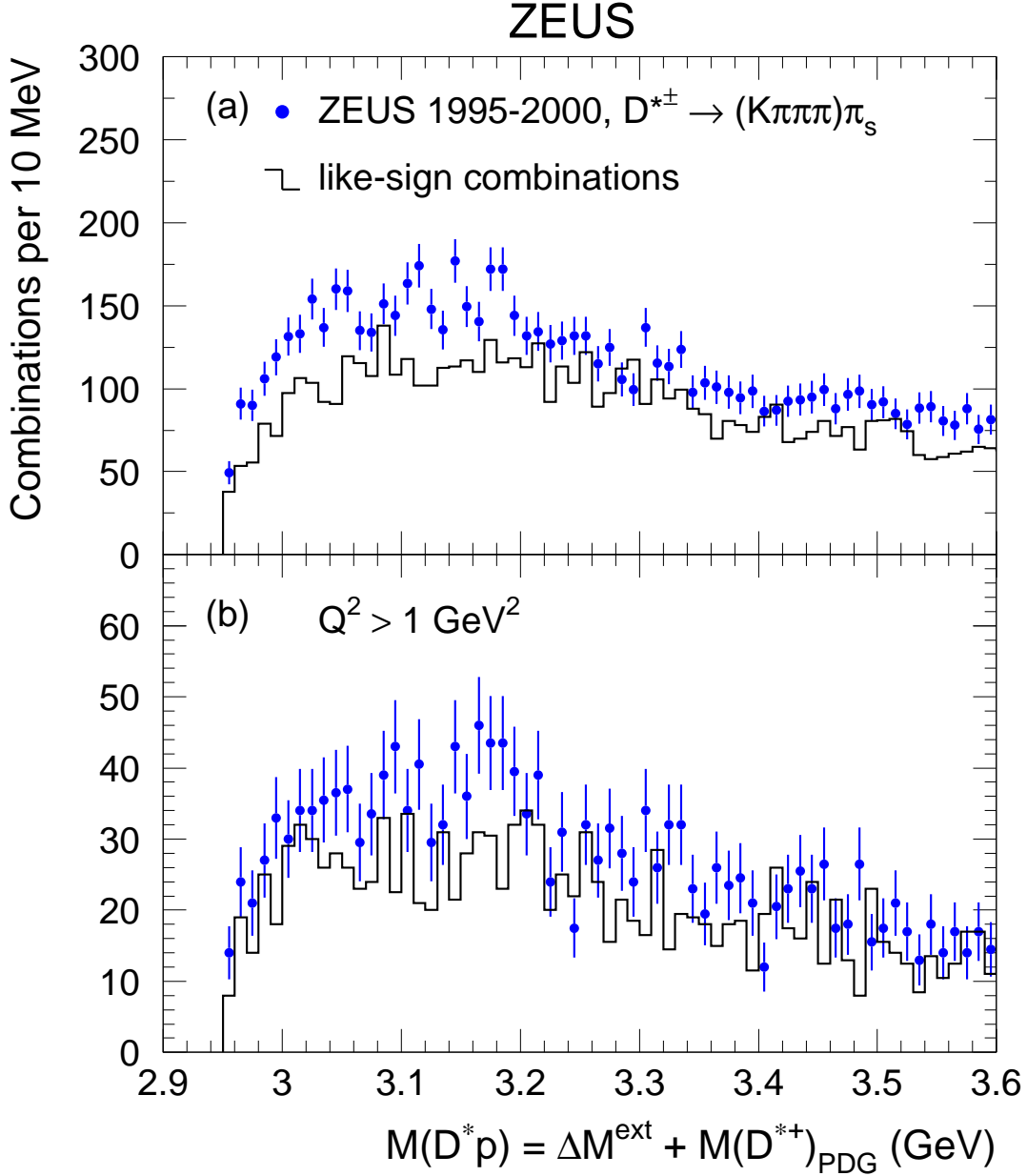


Figure 5: The distribution of $M(D^*p) = \Delta M^{\text{ext}} + M(D^{*+})_{\text{PDG}}$ for charmed pentaquark candidates (dots) (a) in the full data sample and (b) in DIS with $Q^2 > 1 \text{ GeV}^2$. The extended mass difference is defined as $\Delta M^{\text{ext}} = M(K\pi\pi\pi\pi_s p) - M(K\pi\pi\pi\pi_s)$ and $M(D^{*+})_{\text{PDG}}$ is the nominal D^{*+} mass. The histograms show the $M(D^*p)$ distributions for the like-sign combinations.

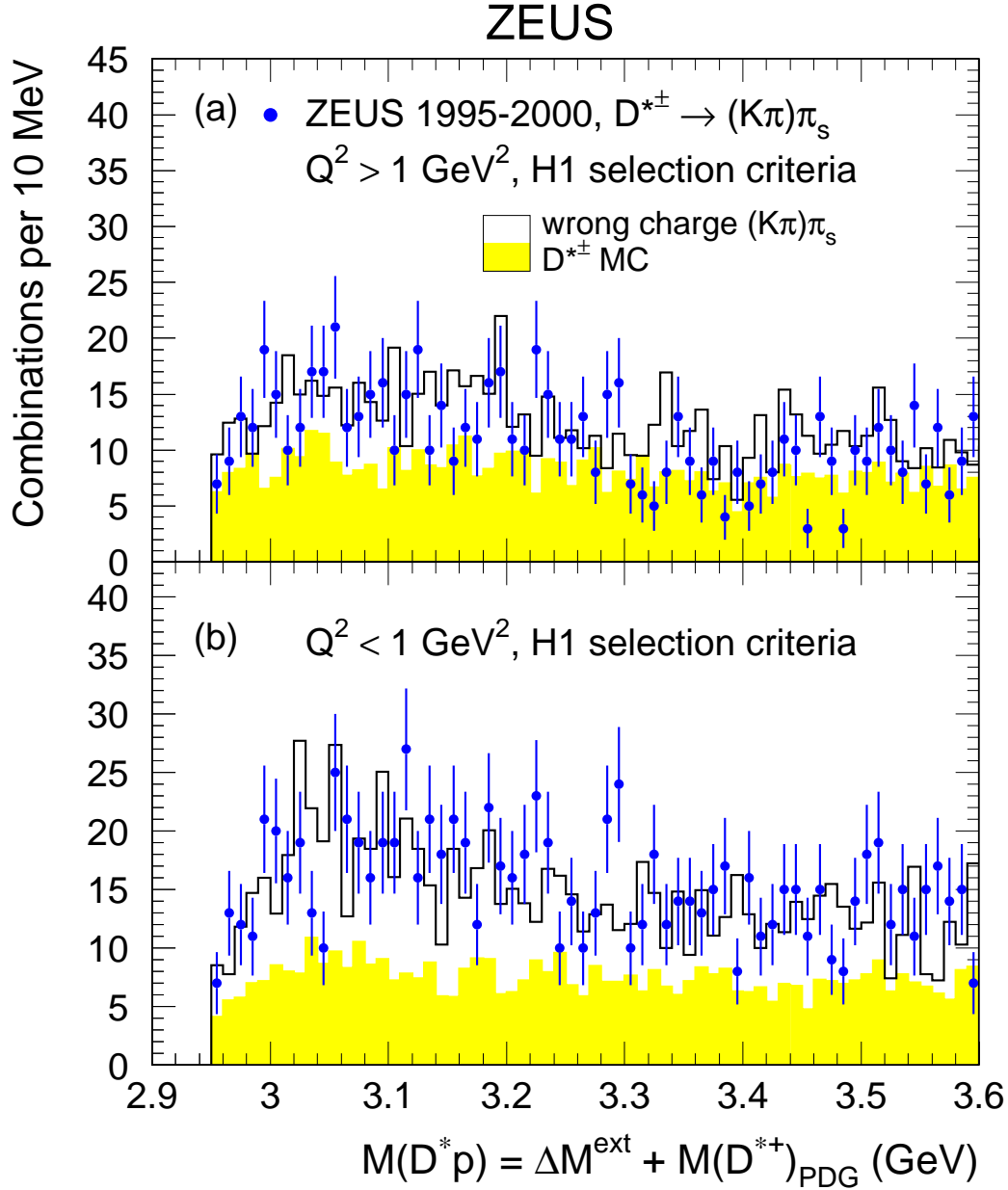


Figure 6: The distribution of $M(D^*p) = \Delta M^{\text{ext}} + M(D^{*+})_{\text{PDG}}$ for charmed pentaquark candidates (dots) obtained using H1 selection criteria in (a) DIS with $Q^2 > 1 \text{ GeV}^2$ and (b) photoproduction with $Q^2 < 1 \text{ GeV}^2$. The extended mass difference is defined as $\Delta M^{\text{ext}} = M(K\pi\pi_s p) - M(K\pi\pi_s)$ and $M(D^{*+})_{\text{PDG}}$ is the nominal D^{*+} mass. The histograms show a two-component model in which the wrong charge $(K\pi)\pi_s$ combinations are used to describe the non-charm contribution and the inclusive $D^{*\pm}$ Monte Carlo simulation (shaded area) describes the contribution of real $D^{*\pm}$ mesons.

ZEUS

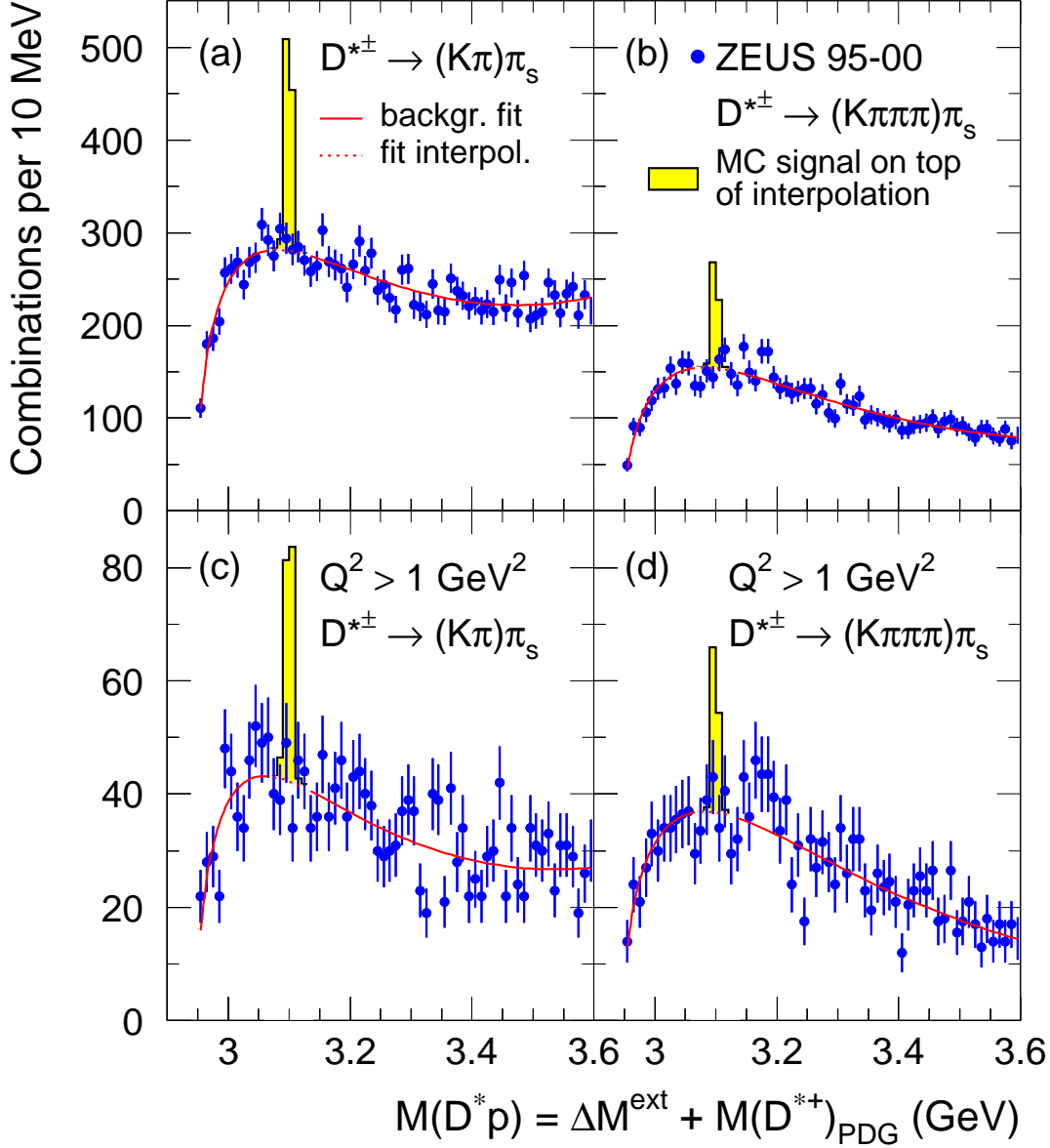


Figure 7: The distribution of $M(D^*p)$ for charmed pentaquark candidates (dots) selected in (a) the full data sample using $D^{*\pm} \rightarrow (K\pi)\pi_s$ candidates, (b) the full data sample using $D^{*\pm} \rightarrow (K\pi\pi\pi)\pi_s$ candidates, (c) DIS with $Q^2 > 1 \text{ GeV}^2$ using $D^{*\pm} \rightarrow (K\pi)\pi_s$ candidates and (d) DIS with $Q^2 > 1 \text{ GeV}^2$ using $D^{*\pm} \rightarrow (K\pi\pi\pi)\pi_s$ candidates. The solid curves are fits to the background function outside the signal window 3.07 – 3.13 GeV. The shaded histograms show the Monte Carlo Θ_c^0 signals, normalised to 1% of the number of reconstructed D^* mesons, and shown on top of the fit interpolations (dashed curves) in the signal window.